STATIONARY PHASE ANALYSIS FOR INTERFEROMETRIC INTERPOLATION APPLIED TO DIPPING REFLECTORS

A. J. O. Pereira and R. Biloti

email: *biloti@ime.unicamp.br*

keywords: *Seismic interferometry, trace interpolation*

ABSTRACT

Seismic Interferometry is a relative new branch of Seismic and Seismology. Despite the start with paper of Claerbout (1968), it was only during the late nineties that the use of Seismic Interferometry start continuously increasing in Seismic. One of the most promising use of this technique is the ability to create new positions of sources and receivers by cross correlating the seismic wavefield recorded. To understand the physical meaning of Seismic Interferometry we study one of its fundamental equations by means of the stationary phase method, in a very simple geometry: a flat dip reflector.

INTRODUCTION

It is possible to define Seismic Interferometry as a variety of methods used to create virtual seismograms, never physically recorded. These virtual seismograms are created only through mathematical operations, which include cross correlation, convolution, deconvolution and summation of actually recorded wavefields, (Galetti and Curtis, 2012). One of the most interesting applications of interferometric methods is the ability to produce artificially traces in positions of sources or receivers that are not possible to be located. With this capacity, at least in principle, it is possible to fill gaps in seismic acquisition (Wang et al., 2009). This possibility is a direct consequence of the nature of physical process behind Seismic Interferometry. In this work, by means of the stationary phase method, we investigate range of applicability of the interferometric interpolation of primary reflections from recorded multiples and primaries. We take the dip of the reflector into account.

SEISMIC INTERFEROMETRY

The retrieval of the Green's Function, or the response of a given media when excited by an impulsive source, is made with interferometric reciprocity equation of correlation type (Wapenaar, 2004; Schuster, 2009), given by

$$\Im\hat{G}(\mathbf{x}_B,\omega;\mathbf{x}_A) = -\omega \oiint_{\varepsilon} \frac{1}{c(\mathbf{x})}\hat{G}(\mathbf{x}_A,\omega;\mathbf{x})\hat{G}^*(\mathbf{x}_B,\omega;\mathbf{x})d\mathbf{S}, \tag{1}$$

where $\Im$ denotes the imaginary part, $\hat{G}(\mathbf{x}_B,\omega;\mathbf{x}_A)$ is the Fourier Transform of the Green's Functions for a source at $\mathbf{x}_A$, evaluated at a receiver at $\mathbf{x}_B$, and ω is the frequency, $\hat{G}^*$ is its complex conjugate, $\mathbf{x}$, the variable of integration, represents source positions over the surface ε, $d\mathbf{S}$ is the element of area, and $c(\mathbf{x})$ is the velocity. The positions $\mathbf{x}_A$ and $\mathbf{x}_B$, where the Green's Functions is computed, are located inside the volume bounded by surface ε. All those elements are sketched on Figure 1.

By means of equation (1), a primary reflection from $\mathbf{x}_A$ to $\mathbf{x}_B$ can be obtained by cross correlating multiple and primary reflections acquired in the field. This is illustrated through a ray diagram, in marine seismic, in Figure 2. In this specific example the dominant arrivals are assumed to be the reflection primaries and free-surface first order multiples. The direct arrivals are muted in the data, an easy task in depth

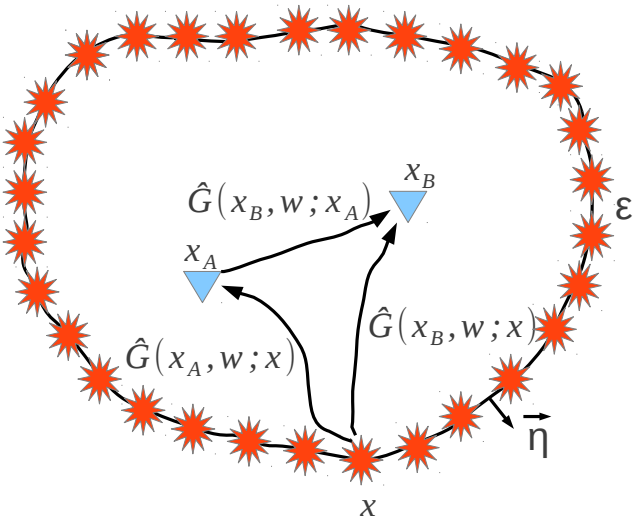

Figure 1: In the figure the rays represent the full response between the source and receivers points, including primary and multiples due to inhomogeneities inside and outside volume (based on Wapenaar and Fokkema (2006)).

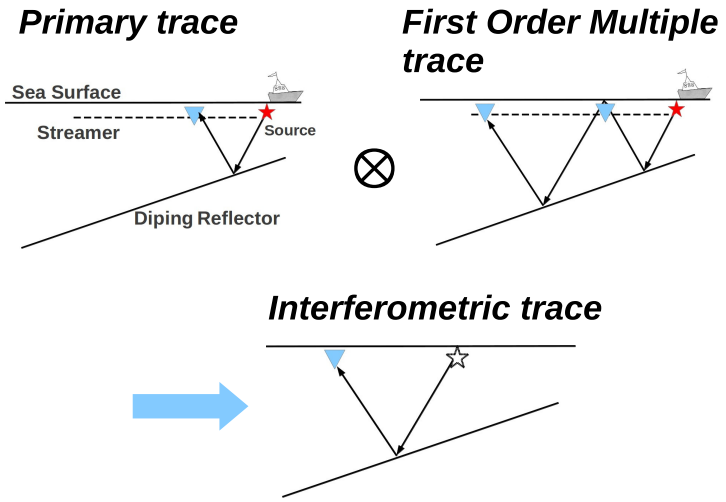

Figure 2: Diagram of cross correlating primaries and multiples from a dipping reflector, modified from Wang et al. (2009). The cross correlation of primaries and first-order multiples results in an interferometric trace.

marine seismic. The Green's function can be approximated as a sum of specular primary reflection and first order multiple reflection. The cross correlation of primaries with primaries or multiples with multiples do not contribute significantly, because as we shall see the stationary contributions of these terms is zero. For a constant velocity overburden, $c(\mathbf{x}) = v$, the Green's Function accounting only for primaries and first order multiples is asymptotically approximated by

$$\hat{G}(\mathbf{x}_M, \omega; \mathbf{x}) \approx \overbrace{r_M \frac{\exp(-i\omega T_{\mathbf{x}\mathbf{x}_M})}{4\pi\, v\, T_{\mathbf{x}\mathbf{x}_M}}}^{Primary} + \overbrace{r'_M \frac{\exp(-i\omega \mathbb{T}_{\mathbf{x}\mathbf{x}_M})}{4\pi\, v\, \mathbb{T}_{\mathbf{x}\mathbf{x}_M}}}^{Multiple}, \tag{2}$$

where r_M and r'_M are the reflection coefficients associated to the primary and multiple reflections, the traveltimes for specular primary reflection and first order free-surface multiple are $T_{\mathbf{x}\,\mathbf{x}_M}$ and $\mathbb{T}_{\mathbf{x}\,\mathbf{x}_M}$, respectively, for source in $\mathbf{x}$, and receiver in $\mathbf{x}_M$ at marine surface.

Suppose that surface $\varepsilon = S_0 + S_\infty$, where S_0 is the surface where the acquisition takes place. Replacing the expression for Green's Function of equation (2) into (1), we obtain

$$\Im\hat{G}(\mathbf{x}_B, \omega; \mathbf{x}_A) \approx \\ -\frac{\omega}{v} r_M r'_M \int_{S_0} \frac{\exp\{-i\omega\,(\mathbb{T}_{\mathbf{x}\,\mathbf{x}_B} - T_{\mathbf{x}\,\mathbf{x}_A})\}}{(4\pi)^2 \mathbb{T}_{\mathbf{x}\,\mathbf{x}_B} T_{\mathbf{x}\,\mathbf{x}_A}} d\mathbf{S} + \mathbf{O}.\mathbf{T}., \tag{3}$$

where O.T. stands for higher order terms, called *virtual multiples* or cross talk, and will be attenuated in the final image for a sufficient large integration's aperture. A last approximation made in equation (3) was to consider that the integral over S_∞ vanishes as its radius goes to infinity. The Figure 3 shows the geometry for this integral.

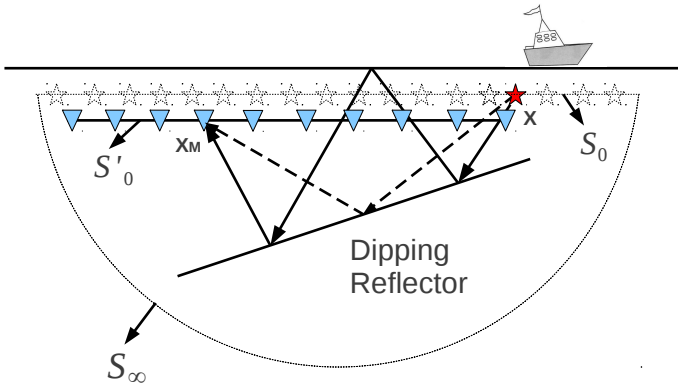

Figure 3: Geometry and surface of integration of equation (3), based on Schuster (2009).

Since the integrand in equation (3) has an oscillatory character, the integral can be asymptotically approximated by the stationary phase method (Bleistein, 1984).

STATIONARY PHASE

The stationary phase method is a method to obtain an asymptotic approximation for integrals with an oscillatory term of the form

$$I = \int_{-\infty}^{\infty} F(x)\, e^{i\omega\phi(x)}\, dx, \tag{4}$$

where ϕ is a rapid varying function of x over most range of integration, and F is a slowly waring function of x. Such kind of integral frequently arise in radiation and scattering problems. Due to the rapid variation of exponential term the integral is approximately zero over all ranges of $\mathbf{x}$, except at regions where $\phi'(x) \approx 0$. Each x^* such that $\phi'(x^*) = 0$, is called an *stationary point* of ϕ. It can be shown (see Bleistein, 1984) that, for large ω, I can be fairly approximated as

$$I \sim \sqrt{\frac{2\pi}{\omega|\phi''(x^*)|}} F(x^*)\, e^{(i\omega\phi(x^*) + i\omega\pi/4)}. \tag{5}$$

This formula states that dominant contribution to the integral comes from point(s) where phase is stationary.

STATIONARY PHASE METHOD IN A PRESENCE OF A DIPPING REFLECTOR

The use stationary phase method to interpret the Seismic Interferometric results in the case of horizontal plane reflectors was done by Snieder (2004), Snieder et al. (2006), and recently by Draganov et al. (2012).

Following the same strategy, we also employ the stationary phase method to investigate if, in the presence of a dipping reflector in a medium of constant velocity, the seismic interferometric interpolation can be useful to create virtual traces.

In our case, the phase function $\phi(x) = \mathbb{T}(x, x_B) - T(x, x_A)$, where x, x_A, and x_B are the horizontal coordinate of points $\mathbf{x}$, $\mathbf{x}_A$, and $\mathbf{x}_B$, respectively, since we are only dealing with 2D acquisition lines, $T(x, x_A)$ is the traveltime of the primary reflection from $\mathbf{x}$ to $\mathbf{x}_A$, and $\mathbb{T}(x, x_B)$ is the traveltime of the first-order multiple reflection from $\mathbf{x}$ to $\mathbf{x}_B$. Note that the primary as well as the multiple reflection have the source at $\mathbf{x}$. Therefore, it would be more suitable to work with a traveltime formula for common shot configuration.

For primary reflections traveltime we will use an expression similar to the one presented on Sheriff and Geldart (1995), pp. 87. To simplify the notation use $T_{x,h}$ to represent the traveltime of a primary reflection from a source at x to a receiver at $2h$ ahead of it, given by

$$T_{x,h} = T_0(x)\sqrt{1 + \frac{h^2 + 2hd(x)\sin\alpha}{d^2(x)}}, \tag{6}$$

where $T_0(x)$ is the traveltime of the zero-offset reflection from the source in x, h is the half-offset, $d_1(x)$ is normal distance from the source to the reflector, α is the dip angle. The zero-offset traveltime and normal distance vary with x as

$$T_0(x) = \frac{2z(x)\cos\alpha}{v} \tag{7}$$

and

$$d(x) = z(x)\cos\alpha, \tag{8}$$

where $z(x)$ is the depth of the dip reflector at x, i.e.,

$$z(x) = z_0 + (x - x_0)\tan\alpha, \tag{9}$$

for some fixed point (x_0, z_0) over the reflector (see Figure 4).

The traveltime of a multiple reflection, in such geometry, is equal to the traveltime of a primary reflection due to a double dip reflector. Therefore, the same expressions just presented by the primary-reflection traveltime can be recasted for the multiple-reflection traveltime:

$$\mathbb{T}_{x,h} = \hat{T}_0(x)\sqrt{1 + \frac{h^2 + 2h\hat{d}(x)\sin 2\alpha}{\hat{d}^2(x)}}, \tag{10}$$

where

$$\hat{T}_0(x) = \frac{2\hat{z}(x)\cos 2\alpha}{v}, \tag{11}$$

and

$$\hat{d}(x) = \hat{z}(x)\cos 2\alpha, \tag{12}$$

where $\hat{z}(x)$ is the depth of the virtual double-dip reflector

$$\hat{z}(x) = \hat{z}_0 + (x - x_0)\tan 2\alpha, \tag{13}$$

with $\hat{z}_0 = z_0(\cos 2\alpha + \sin 2\alpha \tan 2\alpha)$.

From equation (3), the function ϕ, for the stationary phase method, is given by

$$\phi(x) = \mathbb{T}_{x,h} - T_{x,h}. \tag{14}$$

To find the stationary point, representing the sources that contribute most to the integral (3), we have to solve the equation

$$\frac{d\phi(x)}{dx} = 0. \tag{15}$$

Although this equation can not be analytically solved, it is fairly simple to solve it numerically.

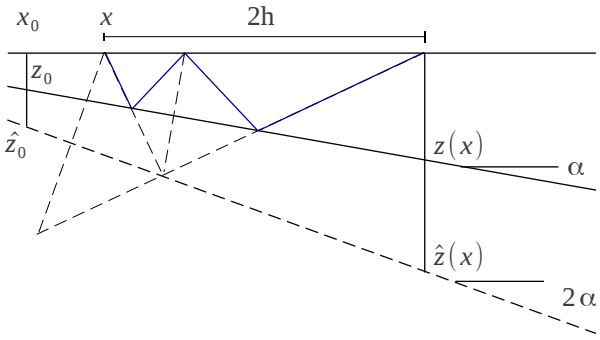

Figure 4: Geometry for the primary and multiple rays.

RESULTS

We present two tests simulating a 2D acquisition line, one for shallow water and another for deeper water. In the case of shallow water, a dipping reflector is located 200 m below receiver in x_A and has 10° dip. The other receiver, x_B, is located 1000 m down dip of the first one, x_A. For this two receivers there is only one stationary point x^* located 292.76 m in shallow water of x_A. Figure 5 shows the situation. As expected, the ray path of the primary from $\mathbf{x}$ to $\mathbf{x}_A$ coincides with the ray path of the first bounce of multiple from $\mathbf{x}$ to $\mathbf{x}_B$.

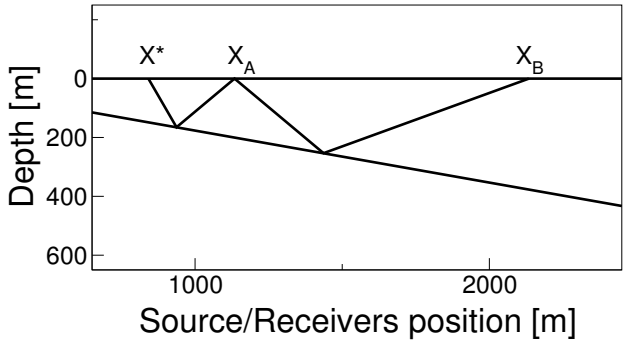

Figure 5: In this shallow water example one receptor is located at 200 m above a dip reflector (10° dip). The stationary point is 292.76 m of x_A. The distance between x_A and x_B is 1000 m.

The second case is a deep water environment, the reflector is 1000 m below the receiver in $\mathbf{x}_A$ and the dip angle is still 10°. The other receiver, x_B, is locate at the same distance of the first one (offset of 1000 m). Again, for this configuration there is only one stationary point x^* at a distance of 161.34 m of x_A (Figure 6).

To investigate how the stationary point moves as the distance of x_A and x_B varies, we present two further results in figures 7 and 8. The horizontal axis is the offset between x_A and x_B. x_A was kept fixed, while x_B was shifted from x_A position up to 8 km, down dip. The vertical axis is the relative position of the stationary source point to the x_A receiver, $(x^* - x_A)$, i.e., negative values stand for stationary points at left of x_A, while positive values stand for stationary points at right of x_A.

For small offsets between x_A and x_B, we can observe that the stationary source points are between the two receivers. Such source–receiver is highly uncommon in conventional towed marine seismic, where all receiver are behind the sources.

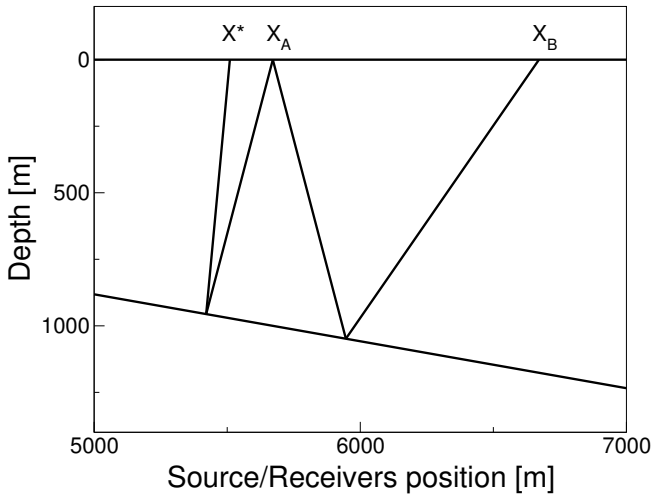

Figure 6: In deep water, one receiver is locate at 1000 m above the same flat dip reflector. The stationary point is only 161.34 m of x_A, in up-dip direction.

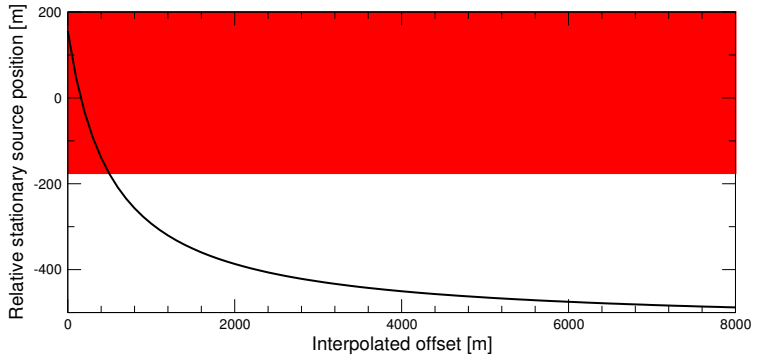

Figure 7: Relative position of the stationary point in the shallow water case.

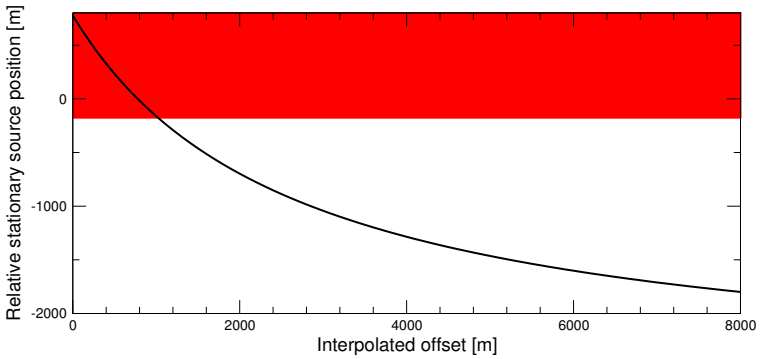

Figure 8: Relative position of the stationary point in the deep water case.

CONCLUSIONS

From the experiments we have made so far, in the shallow water situation we can observe that the predicted positions for stationary sources vary near to the first receiver, up at most 500 m up dip. In the usual

acquisition geometry for towed marine seismic this means that at most 13 shot points, with 25 m between consecutive shots, would be available to span the stationary source positions. The red strip in the Figure 7 indicates the range of offsets between stationary sources and x_A which are not present in the data, due to acquisition constraints. The first trace for which the stationary source would be acquired is the one with offset 500 m, assuming that the minimum recorded offset is 175 m.

In the case of deep water, from Figure 8, we see that the range of positions for stationary sources is more favorable, varying from 175 m up to 1800 m, for 8 km cables. In this range, there is typically 67 shots. Again, the red strip in the figure indicates the range of offsets between sources and x_A which are not present in the data. The first trace for which the stationary source would be acquired is the one with offset 1130 m.

Using stationary-phase method's approach and with the simple geometry of a dip reflector, we were able to investigate what are the most favorable spatial conditions to interpolate traces with Seismic Interferometry. It remains to investigate how much the interpolation actually suffer due to the lack of shots near the stationary source position.

ACKNOWLEDGMENTS

This work was kindly supported by the Brazilian agencies CAPES, FINEP, and CNPq, and the sponsors of the Wave Inversion Technology Consortium.

REFERENCES

Bleistein, N. (1984). *Mathematical Methods for Wave Phenomena*. Academic Press Inc. (Harcort Brace Jovanovich Publishers), New York.

Claerbout, J. F. (1968). Synthesis of layered medium from its acoustic transmission response. *Geophysics*, 33:264–269.

Draganov, D., Heller, K., and Ghose, R. (2012). Monitoring CO2 storage using ghost reflections retrieved from seismic interferometry. *International Journal of Greenhouse Gas Control*, 11:S35–S46.

Galetti, E. and Curtis, A. (2012). Generalised receiver functions and seismic interferometry. *Tectonophysics*, 532-535:1–26.

Schuster, G. T. (2009). *Seismic Interferometry*. Cambridge University Press, Cambridge, UK.

Sheriff, R. E. and Geldart, L. P. (1995). *Exploration Seismology*. Cambridge University Press, Cambridge, 2nd edition.

Snieder, R. (2004). Extracting the Green's function from the correlation of coda waves: A derivation based on stationary phase. *Physical Review E*, 69(4):046610.

Snieder, R., Wapenaar, K., and Larner, K. (2006). Spurious multiples in seismic interferometry of primaries. *Geophysics*, 71:SI111–SI124.

Wang, Y., Luo, Y., and Schuster, G. (2009). Interferometric interpolation of missing data. *Geophysics*, 74:SI37–SI45.

Wapenaar, K. (2004). Retrieving the elastodynamic Green's function of an arbitrary inhomogeneous medium by cross correlation. *Physical Review Letters*, 93:254301–1–254301–4.

Wapenaar, K. and Fokkema, J. (2006). Green's function representations for seismic interferometry. *Geophysics*, 71:SI33–SI46.